Advances in Nano Research, *Vol. 7 No. 3 (2019) 157-167*
DOI: https://doi.org/10.12989/anr.2019.7.3.157

Hygro-thermal effects on wave dispersion responses of magnetostrictive sandwich nanoplates

Farzad Ebrahimi [*1], Ali Dabbagh [1], Francesco Tornabene [2] and Omer Civalek [3]

[1] *Department of Mechanical Engineering, Faculty of Engineering, Imam Khomeini International University, Qazvin, Iran*
[2] *Department of Civil, Chemical, Environmental, and Materials Engineering, University of Bologna, Bologna, Italy*
[3] *Akdeniz University, Engineering Faculty, Civil Engineering Department, Division of Mechanics, 07058 Antalya, Turkey*

(*Received December 20, 2018, Revised March 19, 2019, Accepted April 19, 2019*)

Abstract. In this paper, a classical plate model is utilized to formulate the wave propagation problem of magnetostrictive sandwich nanoplates (MSNPs) while subjected to hygrothermal loading with respect to the scale effects. Herein, magnetostriction effect is considered and controlled on the basis of a feedback control system. The nanoplate is supposed to be embedded on a visco-Pasternak substrate. The kinematic relations are derived based on the Kirchhoff plate theory; also, combining these obtained equations with Hamilton's principle, the local equations of motion are achieved. According to a nonlocal strain gradient theory (NSGT), the small scale influences are covered precisely by introducing two scale coefficients. Afterwards, the nonlocal governing equations can be derived coupling the local equations with those of the NSGT. Applying an analytical solution, the wave frequency and phase velocity of propagated waves can be gathered solving an eigenvalue problem. On the other hand, accuracy and efficiency of presented model is verified by setting a comparison between the obtained results with those of previous published researches. Effects of different variants are plotted in some figures and the highlights are discussed in detail.

Keywords: wave propagation; magnetostrictive materials; nonlocal strain gradient theory (NSGT); sandwich nanoplates; hygro-thermal environments

1. Introduction

As a matter of fact, a giant state of art in smart materials is devoted to the magnetostrictive materials without any exaggeration at all. Actually, these materials are able to exchange magnetic motivations to elastic responses which can be elongation or contraction. It is worth mention that this mentioned magneto-elastic mutual interaction appears as the structure is subjected to a magnetic field. Due to these capabilities, the structures in which possess the magnetostriction effect are excellent candidates for the purpose of being utilized as ultrasonic generators, ultrasonic receivers and echo detectors (Yifeng *et al*. 2013). To this reasons, some of the researchers performed various mechanical analyses on the structures made of such smart materials. Reddy and Barbosa (2000) tried to show how can prevent from vibration in a magnetostrictive composite beam employing both first and third order shear deformation beam models. After about a decade, Hong (2009) presented a new paper dealing with the thermo-mechanical transient dynamic responses of laminated composite plates. The free vibration problem of laminated composite curved beams including magnetostrictive layers is solved by Bayat *et al*. (2015).

Besides, in the recent years, a considerable increasing use of nanosize structures in various nano-electro-mechanical-systems (NEMSs) is observed which makes it obligatory for designers to earn reliable information about the mechanical characteristics of structures in small scales. Hence, classical continuum theories must be replaced by size-dependent continuum theories to take into consider the scale effects once analyzing the nano-mechanical responses of elements. To this reason, Eringen (1983) presented the first nonlocal continuum theory, called nonlocal elasticity theory (NET). Hitherto, lots of authors performed their researches on the nanostructures in the framework of this theory. Natarajan *et al*. (2012) could show the scale effects while studying the dynamic behaviors of small composite plates based on the NET. Also, the NE is utilized by Hosseini-Hashemi *et al*. (2013) to survey the vibration problem of nanosize plates with respect to shear deformation applying a first-order shear deformable plate model. Moreover, Yan *et al*. (2015) captured the small scale influences in the framework of the NE while investigating the bending characteristics of nano scale beams and plates. Ebrahimi *et al*. (2015) used the NET to analyze the thermo-elastic vibrational characteristics of nanobeams. The effect of exact position of the neutral axis of a composite nanobeam on the dynamic responses of this nanostructure is considered by Ahouel *et al*. (2016) within the framework of the nonlocal hypothesis of Eringen. In addition, Ebrahimi and Hosseini (2016) studied the vibration problem of viscoelastic double-layered nanoplates once both thermal and small scale effects are considered. Moreover, the stability behaviors of composite nanobeams in hygro-thermal environments and under an induced magnetic force

*Corresponding author, Associate Professor,
E-mail: febrahimy@gmail.com

ISSN: 2287-237X (Print), 2287-2388 (Online)

are investigated by Ebrahimi and Barati (2016) according to the NET. The effects of small scale are considered by Bellifa *et al*. (2017) in an article dealing with the nonlocal post-buckling responses of nanobeams. Besides, (Mouffoki *et al*. 2017) have probed the hygro-thermally influenced dynamic characteristics of nanobeams via a new two-variable kinematic theorem. Hamza-Cherif *et al*. (2018) utilized a powerful numerical method for the goal of analyzing the thermally affected vibrational behaviors of carbon nanotubes simulated with a nanobeam. On the other hand, some of the scientific works deal with the efficiency of the size-dependent continuum theories. In fact, in the some of the published researches it is proven that the NET of Eringen is not able to cover the scale effects completely (Fleck and Hutchinson 1993, Stölken and Evans 1998). Actually, according to the NE, nonlocality results in a decreasing effect on the mechanical responses of nanosize structures; whereas, the scale influences cannot be summarized in the framework of this decreasing impact. In other words, there is a totally different increasing effect which is predicted in the strain gradient elasticity which is neglected in the NE. Lately, Lim *et al*. (2015) tried to combine these effects to present a general theory which is efficient enough to take into account for both of the mentioned effects. In this new theory, named nonlocal strain gradient theory (NSGT), two scale coefficients are introduced to capture both diminishing and strengthening impacts of small size. Li and Hu (2015) tried to highlight the effects of strain gradient stress field on the buckling responses of geometrically nonlinear nanobeams. The buckling characteristics of NSG based orthotropic graphene sheets are considered by Farajpour *et al*. (2016). In addition, Ebrahimi and Barati (2018b) have investigated the dynamic behaviors of graphene sheets embedded on an orthotropic elastic medium under hygro-thermo-magnetic loadings via a NSGT. Besides, Ebrahimi *et al*. (2017) presented a NSGT for wave propagation analysis of compositionally graded nanobeams in thermal environments. Also, Ebrahimi and Barati (2017) surveyed the thermo-magneto-elastic dynamic responses of axially graded nanosize beams based on the NSGT. In another paper, Li *et al*. (2018b) have surveyed the nonlinear natural frequency behaviors of a porous nanobeam by the means of the NSGT by considering the effect of existence of an imperfection. The dynamic responses of double-layered viscoelastic graphene sheets are reviewed by Ebrahimi and Barati (2018a) on the basis of a NSGT coupled with a refined higher-order shear deformable two-variable plate theory. Lately, Karami *et al*. (2019) probed the effects of hygro-thermal environments on the dispersion characteristics of a porous nanobeam whenever the effects of magnetic field on the nanostructure are included.

In the recent years, a remarkable interest in the science society is allocated to the static and dynamic analyses of tiny structures, whereas, the wave propagation problem of such small scale elements has never been mentioned a lot. Only a few researches can be found about the dispersion characteristics of waves propagating through an element. Ebrahimi and his co-workers performed their researches on the wave dispersion answers of composite nanosize beams and plates under various thermo-electro-magneto-elastic loadings via different nonlocal continuum theories (Ebrahimi *et al*. 2016a, b, c, 2018a, b, Ebrahimi and Dabbagh 2017a, b, c, d, 2018a, b, c, e, f). Ghorbanpour Arani *et al*. (2017) studied the wave propagation behaviors of viscoelastic sandwich nanoplates with respect to surface effects and smart properties of nanoplate. In another attempt, Xiao *et al*. (2017) examined the wave propagation characteristics of monolayer graphene sheets via a NSG based plate model. Karami *et al*. (2018) employed the NSGT incorporated with the higher-order kinematic hypothesis of doubly-curved nanoshells in order to study the wave propagation problem of such nanostructures. Ebrahimi and Dabbagh (2018g) tried to examine the wave propagation problem of a magneto-strictive sandwich nanoplate (MSNP) incorporating nonlocal stress-strain gradient elasticity theory. In the most recent research in this area, Ebrahimi and Dabbagh (2018d) probed the wave propagation problem of a MSNP in thermal environments subjected to an external induced magnetic force. It can be figured out that the issue of analyzing the wave dispersion problem in the nanosize MS structures must be investigated more than before. Indeed, only two papers can be found dealing with the wave propagation features of MSNPs. Obviously, it can be easily found that the wave dispersion responses of MSNPs once subjected to hygro-thermal loadings has never been surveyed up to now.

Present work is going to solve this lack of information about the hygro-thermo-elastic wave propagation characteristics of MSNPs employing a NSG plate model. The displacement fields of the SNP are assumed to be derived applying the kinematic relations of classical plate theory (CPT). Furthermore, the system is considered to be rested on a viscoelastic medium which is made of Winkler, Pasternak and damping coefficients. According to a Hamiltonian approach, the Euler-Lagrange equations are reached. The magnetostriction impact is controlled via a feedback control system. The nonlocal governing equations are solved analytically and the wave frequency and phase velocity values are obtained. At the end, effect of different parameters is highlighted in some separate diagrams.

2. Theory and formulation

2.1 Stress-strain relations for magnetostrictive materials

The relation between stress, strain and magnetic field can be explained for magnetostrictive materials as Ebrahimi and Dabbagh (2018g)

$$\sigma_{xx} = C_{11}\varepsilon_{xx} + C_{12}\varepsilon_{yy} - e_{31}H_z \tag{1}$$

$$\sigma_{yy} = C_{21}\varepsilon_{xx} + C_{22}\varepsilon_{yy} - e_{32}H_z \tag{2}$$

$$\sigma_{xy} = C_{66}\varepsilon_{xy} - e_{34}H_z \tag{3}$$

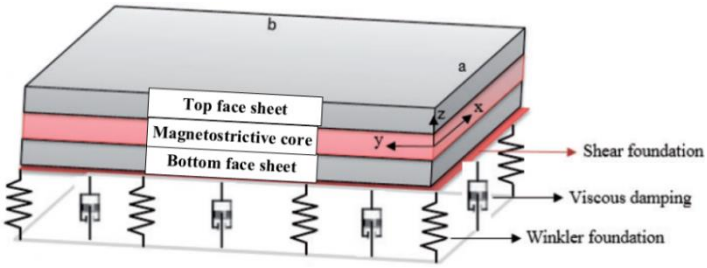

Fig. 1 Schematic of a MSNP rested on a visco-Pasternak medium

where σ_{ij}, ε_{ij}, e_{ij} and H_z denote stress, strain, magnetostrictive constant and magnetic field, respectively.

In addition, C_{ij} stand for the elastic stiffness coefficient which are defined as Ebrahimi and Dabbagh (2018g)

$$C_{11}=C_{22}=\frac{E_c}{1-\nu_c^{\,2}},\quad C_{12}=\frac{\nu_c E_c}{1-\nu_c^{\,2}},\quad C_{66}=\frac{E_c}{2(1+\nu_c)} \tag{4}$$

in which E_c and ν_c denote the modulus of elasticity and Poisson's ratio of the core, respectively. Here, it is interesting to inform about a reciprocal magneto-elastic interaction which is available in magnetostrictive materials. Indeed, such materials are able to tolerate elongation or compression once subjected to a magnetic field. This phenomenon is reported to be induced due to the reorientation of the atomic magnetic moments (Reddy and Barbosa 2000). Moreover, on the basis of a feedback control system it is tried to account for the intensity of magnetic field for the goal of capturing the magnetization effect in MSCNP. According to this model as illustrated in Fig. 1, the magnetostrictive coefficients can be easily formulated in the following (Ebrahimi and Dabbagh 2018g)

$$e_{31}=\tilde{e}_{31}\cos^2\psi+\tilde{e}_{32}\sin^2\psi \tag{5}$$

$$e_{32}=\tilde{e}_{32}\cos^2\psi+\tilde{e}_{31}\sin^2\psi \tag{6}$$

in which Ψ denotes the angle that the magnetic anisotropy might be induced. In the present research, a unidirectional magnetic field along z axis is utilized to be applied to the MSCNP to account for the magnetization effects. Now, the magnetic field intensity can be expressed as follows (Ebrahimi and Dabbagh 2018g)

$$H_z=K_c I(x,y,t)=K_c C(t)\frac{\partial w(x,y,t)}{\partial t} \tag{7}$$

in which K_c is the coil constant which is a function of the coil characteristics such as its width, radius and number of turns of the coil. Actually, coil constant can be formulated as (Ebrahimi and Dabbagh 2018g, Reddy and Barbosa 2000)

$$K_c=\frac{n_c}{\sqrt{b_c^{\,2}+4r_c^{\,2}}} \tag{8}$$

where n_c, b_c and r_c are related to turns of coil, coil width and coil radius, respectively. Besides, $I(t)$ and $C(t)$ stand for the coil current and control gain, respectively. It shall be considered that the control gain is presumed to be constant. Finally, $K_c\,C(t)$ is the velocity feedback gain.

On the other hand, the stress-strain relations of the top and bottom layers are going to be explained. As same as the central core, here, for the upper and lower face sheets the above equations are employed (Ebrahimi and Dabbagh 2018g)

$$\sigma_{xx}=Q_{11}\varepsilon_{xx}+Q_{12}\varepsilon_{yy} \tag{9}$$

$$\sigma_{yy}=Q_{21}\varepsilon_{xx}+Q_{22}\varepsilon_{yy} \tag{10}$$

$$\sigma_{xy}=Q_{66}\varepsilon_{xy} \tag{11}$$

where

$$Q_{11}=\frac{E_f}{1-\nu_f^{\,2}},\quad Q_{12}=\frac{\nu_f E_f}{1-\nu_f^{\,2}},\quad Q_{22}=\frac{E_f}{1-\nu_f^{\,2}},\quad Q_{66}=\frac{E_f}{2(1+\nu_f)} \tag{12}$$

in which E_f is Young's modulus and ν_f is Poisson's ratios.

2.2 Kinematic relations

The equations of motion for the plates are modeled in the present research according to the classical plate theory in the following form (Ebrahimi and Dabbagh 2018g)

$$u_x(x,y,z,t)=u(x,y,t)-z\frac{\partial w(x,y,t)}{\partial x} \tag{13}$$

$$u_y(x,y,z,t)=v(x,y,t)-z\frac{\partial w(x,y,t)}{\partial y} \tag{14}$$

$$u_z(x,y,z,t)=w(x,y,t) \tag{15}$$

in which, u, v and w correspond with the displacement components in the x, y and z directions, respectively. In this study, the influences of shear stress and strain are ignored, however, one can reach more information about this issue by reading complementary references (Abdelaziz *et al.* 2017, Beldjelili *et al.* 2016). Besides, whenever the effects of the thickness stretching are of importance, the researchers are advised to employ the quasi-3D models instead of the conventional ones. One can obtain more

detailed data by looking at the references in this field (Zaoui *et al*. 2019, Abualnour *et al*. 2018). Therefore, the nonzero strains of the core plate can be defined as (Ebrahimi and Dabbagh 2018g)

$$\begin{Bmatrix} \varepsilon_{xx}^{core} \\ \varepsilon_{yy}^{core} \\ \varepsilon_{xy}^{core} \end{Bmatrix} = \begin{Bmatrix} \varepsilon_{xx}^{core} \\ \varepsilon_{yy}^{core} \\ \varepsilon_{xy}^{core} \end{Bmatrix} + z \begin{Bmatrix} \kappa_{xx}^{core} \\ \kappa_{yy}^{core} \\ \kappa_{xy}^{core} \end{Bmatrix} \tag{16}$$

where

$$\begin{Bmatrix} \varepsilon_{xx}^{core} \\ \varepsilon_{yy}^{core} \\ \varepsilon_{xy}^{core} \end{Bmatrix} = \begin{Bmatrix} \dfrac{\partial u}{\partial x} \\ \dfrac{\partial v}{\partial y} \\ \dfrac{\partial u}{\partial y} + \dfrac{\partial v}{\partial x} \end{Bmatrix}, \quad \begin{Bmatrix} \kappa_{xx}^{core} \\ \kappa_{yy}^{core} \\ \kappa_{xy}^{core} \end{Bmatrix} = \begin{Bmatrix} -\dfrac{\partial^2 w}{\partial x^2} \\ -\dfrac{\partial^2 w}{\partial y^2} \\ -2\dfrac{\partial^2 w}{\partial x \partial y} \end{Bmatrix} \tag{17}$$

Moreover, for the face sheets the same relations can be developed (Ebrahimi and Dabbagh 2018g)

$$\begin{Bmatrix} \varepsilon_{xx}^{face} \\ \varepsilon_{yy}^{face} \\ \varepsilon_{xy}^{face} \end{Bmatrix} = \begin{Bmatrix} \varepsilon_{xx}^{face} \\ \varepsilon_{yy}^{face} \\ \varepsilon_{xy}^{face} \end{Bmatrix} + z \begin{Bmatrix} \kappa_{xx}^{face} \\ \kappa_{yy}^{face} \\ \kappa_{xy}^{face} \end{Bmatrix} \tag{18}$$

where

$$\begin{Bmatrix} \varepsilon_{xx}^{face} \\ \varepsilon_{yy}^{face} \\ \varepsilon_{xy}^{face} \end{Bmatrix} = \begin{Bmatrix} \dfrac{\partial u}{\partial x} \\ \dfrac{\partial v}{\partial y} \\ \dfrac{\partial u}{\partial y} + \dfrac{\partial v}{\partial x} \end{Bmatrix}, \quad \begin{Bmatrix} \kappa_{xx}^{face} \\ \kappa_{yy}^{face} \\ \kappa_{xy}^{face} \end{Bmatrix} = \begin{Bmatrix} -\dfrac{\partial^2 w}{\partial x^2} \\ -\dfrac{\partial^2 w}{\partial y^2} \\ -2\dfrac{\partial^2 w}{\partial x \partial y} \end{Bmatrix} \tag{19}$$

Also, it is interesting that in some of the papers, researchers select a new version of the classical beam or plate models that are modified in a way that can capture the effect of shear deformation (Kaci *et al*. 2018, Zidi *et al*. 2017, Houari *et al*. 2016). Now, according to the Hamilton's principle the Euler-Lagrange equations of the MSP as follows (Ebrahimi and Barati 2018b)

$$\int_0^t \delta(U - T + V)dt = 0 \tag{20}$$

where *U*, *T* and *V* account for strain energy, kinetic energy and work done by external forces, respectively. Now, the variation of strain energy for core and face sheets can be formulated as (Ebrahimi and Dabbagh 2018g)

$$\delta U^{core} = \int_0^a \begin{pmatrix} N_{xx}^{core}\left(\delta\varepsilon_{xx}^{core}\right) + M_{xx}^{core}\left(\delta\kappa_{xx}^{core}\right) + \\ N_{yy}^{core}\left(\delta\varepsilon_{yy}^{core}\right) + M_{yy}^{core}\left(\delta\kappa_{yy}^{core}\right) + \\ N_{xy}^{core}\left(\delta\varepsilon_{xy}^{core}\right) + M_{xy}^{core}\left(\delta\kappa_{xy}^{core}\right) \end{pmatrix} dx \tag{21}$$

$$\delta U^{face} = \int_0^a \begin{pmatrix} N_{xx}^{face}\left(\delta\varepsilon_{xx}^{face}\right) + M_{xx}^{face}\left(\delta\kappa_{xx}^{face}\right) + \\ N_{yy}^{face}\left(\delta\varepsilon_{yy}^{face}\right) + M_{yy}^{face}\left(\delta\kappa_{yy}^{face}\right) + \\ N_{xy}^{face}\left(\delta\varepsilon_{xy}^{face}\right) + M_{xy}^{face}\left(\delta\kappa_{xy}^{face}\right) \end{pmatrix} dx \tag{22}$$

in above equation, the axial forces and bending moments can be defined as (Ebrahimi and Dabbagh 2018g)

$$\left(N_{ij}^{core}, M_{ij}^{core}\right) = \int_{-\frac{h_c}{2}}^{\frac{h_c}{2}} \int_0^b (1, z)\sigma_{ij}^{core} dydz, \quad (i, j = x, y) \tag{23}$$

$$\begin{aligned} \left(N_{ij}^{face}, M_{ij}^{face}\right) = \Bigg(& \int_{-\frac{\left(h_c+h_f\right)}{2}}^{-\frac{h_c}{2}} \int_0^b (1, z)\sigma_{ij}^{face} dydz \\ & + \int_{\frac{h_c}{2}}^{\frac{\left(h_c+h_f\right)}{2}} \int_0^b (1, z)\sigma_{ij}^{face} dydz \Bigg), \quad (i, j = x, y) \end{aligned} \tag{24}$$

Also, the variation of kinetic energy can be expressed as follows (Ebrahimi and Dabbagh 2018g)

$$\begin{aligned} \delta T = \int_0^L \Bigg(& I_0 \left(\frac{\partial u}{\partial t}\frac{\partial \delta u}{\partial t} + \frac{\partial v}{\partial t}\frac{\partial \delta v}{\partial t} + \frac{\partial w}{\partial t}\frac{\partial \delta w}{\partial t} \right) \\ & + I_2 \left(\frac{\partial^2 w}{\partial x \partial t}\frac{\partial^2 \delta w}{\partial x \partial t} + \frac{\partial^2 w}{\partial y \partial t}\frac{\partial^2 \delta w}{\partial y \partial t} \right) \Bigg) dx \end{aligned} \tag{25}$$

in which, the mass moments of inertia are defined as (Ebrahimi and Dabbagh 2018g)

$$I_0 = \int_{-\frac{h_c}{2}}^{\frac{h_c}{2}} \int_0^b \rho_c dydz + \left(\int_{-\frac{\left(h_c+h_f\right)}{2}}^{-\frac{h_c}{2}} \int_0^b \rho_f dydz + \int_{\frac{h_c}{2}}^{\frac{\left(h_c+h_f\right)}{2}} \int_0^b \rho_f dydz \right) \tag{26}$$

$$I_2 = \int_{-\frac{h_c}{2}}^{\frac{h_c}{2}} \int_0^b \rho_c z^2 dydz + \left(\int_{-\frac{\left(h_c+h_f\right)}{2}}^{-\frac{h_c}{2}} \int_0^b \rho_f z^2 dydz + \int_{\frac{h_c}{2}}^{\frac{\left(h_c+h_f\right)}{2}} \int_0^b \rho_f z^2 dydz \right) \tag{27}$$

where ρ_c and ρ_f correspond with the density of the core plate and face sheets, respectively. Now, the variation of the external work done by external forces can be written in the following form (Ebrahimi and Dabbagh 2018g, Ebrahimi and Barati 2018b)

$$\begin{aligned} \delta V = \int_0^L \Bigg(& -k_w \delta w + k_p \left(\frac{\partial^2 \delta w}{\partial x^2} + \frac{\partial^2 \delta w}{\partial y^2} \right) - c_d \frac{\partial w}{\partial t} \\ & - \left(N^T + N^H \right) \left(\frac{\partial^2 \delta w}{\partial x^2} + \frac{\partial^2 \delta w}{\partial y^2} \right) \Bigg) dx \end{aligned} \tag{28}$$

where k_w, k_p and c_d are Winkler, Pasternak and damping coefficients of elastic medium, respectively. Also, N^T and N^H stand for the applied loads due to the temperature rise and moisture concentration, respectively. Herein, once Eqs. (21), (22), (25) and (28) are substituted in Eq. (20) and the coefficients of δu, δv and δw are set to zero, the Euler-Lagrange equations of MSCPs can be written as follows (Ebrahimi and Dabbagh 2018g, Ebrahimi and Barati 2018b)

$$\frac{\partial N_{xx}}{\partial x}+\frac{\partial N_{xy}}{\partial y}=I_0\frac{\partial^2 u}{\partial t^2}+\frac{e_{31}K_cC(t)h_c}{E_c}\frac{\partial^2 w}{\partial x\partial t} \tag{29}$$

$$\frac{\partial N_{xy}}{\partial x}+\frac{\partial N_{yy}}{\partial y}=I_0\frac{\partial^2 v}{\partial t^2}+\frac{e_{32}K_cC(t)h_c}{E_c}\frac{\partial^2 w}{\partial y\partial t} \tag{30}$$

$$\begin{aligned}&\frac{\partial^2 M_{xx}}{\partial x^2}+2\frac{\partial^2 M_{xy}}{\partial x\partial y}+\frac{\partial^2 M_{yy}}{\partial y^2}-\left(N^T+N^H\right)\nabla^2 w\\&=I_0\frac{\partial^2 w}{\partial t^2}-I_2\nabla^2\frac{\partial^2 w}{\partial t^2}+k_w w-k_p\nabla^2 w+c_d\frac{\partial w}{\partial t}\\&\quad+\frac{e_{31}K_cC(t)h_c}{E_c}\frac{\partial^2 u}{\partial x\partial t}+\frac{e_{32}K_cC(t)h_c}{E_c}\frac{\partial^2 v}{\partial y\partial t}\end{aligned} \tag{31}$$

2.3 Nonlocal strain gradient elasticity

According to this theory, two nonlocal and length scale parameters should be included in an efficient theory which is powerful enough to take into consider the scale influences. So, the initial form of this theory can be expressed as (Ebrahimi *et al*. 2016a)

$$\sigma_{ij}=\sigma_{ij}^{(0)}-\frac{d\sigma_{ij}^{(1)}}{dx} \tag{32}$$

where $\sigma_{ij}^{(0)}$ and $\sigma_{ij}^{(1)}$ are classical and higher order stresses which are related to the strain (ε_{xx}) and strain gradient ($\varepsilon_{xx,x}$), respectively. These stresses can be formulated as Ebrahimi *et al*. (2016a)

$$\sigma_{ij}^{(0)}=\int_0^L C_{ijkl}\alpha_0(x,x',e_0a)\varepsilon'_{kl}(x')dx' \tag{33}$$

$$\sigma_{ij}^{(1)}=l^2\int_0^L C_{ijkl}\alpha_1(x,x',e_1a)\varepsilon'_{kl,x}(x')dx' \tag{34}$$

in which C_{ijkl} is the elastic coefficient; e_0a and e_1a are introduced to account for the nonlocality effects. Also, l captures the strain gradient effects. Once the nonlocal kernel functions α_0 (x, x', e_0a) and α_1 (x, x', e_1a) satisfy the developed conditions, the constitutive relation of nonlocal strain gradient theory can be expressed as below (Ebrahimi *et al*. 2016a)

$$\begin{aligned}&\left(1-(e_1a)^2\nabla^2\right)\left(1-(e_0a)^2\nabla^2\right)\sigma_{ij}\\&=C_{ijkl}\left(1-(e_1a)^2\nabla^2\right)\varepsilon_{kl}-C_{ijkl}\,l^2\left(1-(e_0a)^2\nabla^2\right)\nabla^2\varepsilon_{kl}\end{aligned} \tag{35}$$

in which ∇^2 denotes the Laplacian operator. Considering $e_1 = e_0 = e$, the general constitutive relation in Eq. (35) can be stated as follows with respect to hygrothermal influences (Ebrahimi and Barati 2018b, Ebrahimi *et al*. 2016a)

$$\left(1-\mu^2\nabla^2\right)\sigma_{ij}=C_{ijkl}\left(1-\lambda^2\nabla^2\right)\left(\varepsilon_{kl}-\alpha_{ij}T-\beta_{ij}C\right) \tag{36}$$

where $\mu = ea$ and $\lambda = l$ are nonlocal and length scale parameters, respectively. Furthermore, α_{ij} and β_{ij} denote the thermal and moisture expansion coefficients, respectively; also, T and C stand for temperature in terms of Kelvin degrees and moisture concentration, respectively. It is worth mentioning that in some cases, the effect of the Poisson's ratio and the structures' thickness on the constitutive behaviors of nanostructures are studied (Tang *et al*. 2019, Li *et al*. 2018a). Now, the final nonlocal relations of normal forces and bending moments can be achieved by integrating from Eq. (36) over the cross section area of the plate as (Ebrahimi and Dabbagh 2018g)

$$\begin{aligned}&\left(1-\mu^2\nabla^2\right)\begin{bmatrix}N_{xx}\\N_{yy}\\N_{xy}\end{bmatrix}\\&=\left(1-\lambda^2\nabla^2\right)\left(\begin{bmatrix}A_{11}&A_{12}&0\\A_{21}&A_{22}&0\\0&0&A_{66}\end{bmatrix}\begin{bmatrix}\frac{\partial u}{\partial x}\\\frac{\partial v}{\partial y}\\\frac{\partial u}{\partial y}+\frac{\partial v}{\partial x}\end{bmatrix}+\begin{bmatrix}B_{11}&B_{12}&0\\B_{21}&B_{22}&0\\0&0&B_{66}\end{bmatrix}\begin{bmatrix}-\frac{\partial^2 w}{\partial x^2}\\-\frac{\partial^2 w}{\partial y^2}\\-2\frac{\partial^2 w}{\partial x\partial y}\end{bmatrix}\right)\end{aligned} \tag{38}$$

$$\begin{aligned}&\left(1-\mu^2\nabla^2\right)\begin{bmatrix}M_{xx}\\M_{yy}\\M_{xy}\end{bmatrix}\\&=\left(1-\lambda^2\nabla^2\right)\left(\begin{bmatrix}B_{11}&B_{12}&0\\B_{21}&B_{22}&0\\0&0&B_{66}\end{bmatrix}\begin{bmatrix}\frac{\partial u}{\partial x}\\\frac{\partial v}{\partial y}\\\frac{\partial u}{\partial y}+\frac{\partial v}{\partial x}\end{bmatrix}+\begin{bmatrix}D_{11}&D_{12}&0\\D_{21}&D_{22}&0\\0&0&D_{66}\end{bmatrix}\begin{bmatrix}-\frac{\partial^2 w}{\partial x^2}\\-\frac{\partial^2 w}{\partial y^2}\\-2\frac{\partial^2 w}{\partial x\partial y}\end{bmatrix}\right)\end{aligned} \tag{37}$$

where

$$\begin{aligned}&\begin{bmatrix}A_{11}&B_{11}&D_{11}\\A_{22}&B_{22}&D_{22}\\A_{12}&B_{12}&D_{12}\\A_{66}&B_{66}&D_{66}\end{bmatrix}=\int_{-\frac{h_c}{2}}^{\frac{h_c}{2}}\int_0^b\begin{bmatrix}1&z&z^2\end{bmatrix}\begin{bmatrix}C_{11}\\C_{22}\\C_{12}\\C_{66}\end{bmatrix}dydz\\&+\int_{-\frac{\left(h_c+h_f\right)}{2}}^{\frac{-h_c}{2}}\int_0^b\begin{bmatrix}1&z&z^2\end{bmatrix}\begin{bmatrix}Q_{11}\\Q_{22}\\Q_{12}\\Q_{66}\end{bmatrix}dydz\\&S_{21}=S_{12},\qquad\left(S=A,B,D\right)\end{aligned} \tag{39}$$

Now, the final governing equations of MSNPs can be achieved by substituting Eqs. (37) and (38) in Eqs. (29)-(31)

$$\left(1-\lambda^2\nabla^2\right)\left(A_{11}\frac{\partial^2 u}{\partial x^2}+\left(A_{12}+A_{66}\right)\frac{\partial^2 v}{\partial x\partial y}+A_{66}\frac{\partial^2 u}{\partial y^2}\right. \tag{40}$$

$$-B_{11}\frac{\partial^3 w}{\partial x^3}-\left(B_{12}+2B_{66}\right)\frac{\partial^3 w}{\partial x\partial y^2}\Bigg)+\left(1-\mu^2\nabla^2\right)\left(-I_0\frac{\partial^2 u}{\partial t^2}-\frac{e_{31}K_cC(t)h_c}{E_c}\frac{\partial^2 w}{\partial x\partial t}\right)=0 \tag{40}$$

$$\left(1-\lambda^2\nabla^2\right)\left(A_{22}\frac{\partial^2 v}{\partial y^2}+\left(A_{12}+A_{66}\right)\frac{\partial^2 u}{\partial x\partial y}+A_{66}\frac{\partial^2 v}{\partial x^2}-B_{22}\frac{\partial^3 w}{\partial y^3}-\left(B_{12}+2B_{66}\right)\frac{\partial^3 w}{\partial x^2\partial y}\right)+\left(1-\mu^2\nabla^2\right)\left(-I_0\frac{\partial^2 v}{\partial t^2}-\frac{e_{32}K_cC(t)h_c}{E_c}\frac{\partial^2 w}{\partial y\partial t}\right)=0 \tag{41}$$

$$\begin{gathered}\left(1-\lambda^2\nabla^2\right)\left(\begin{array}{c}B_{11}\frac{\partial^3 u}{\partial x^3}+\left(B_{12}+2B_{66}\right)\frac{\partial^3 u}{\partial x\partial y^2}+B_{22}\frac{\partial^3 v}{\partial y^3}+\left(B_{12}+2B_{66}\right)\frac{\partial^3 v}{\partial x^2\partial y}\\ -D_{11}\frac{\partial^4 w}{\partial x^4}-2\left(D_{12}+2D_{66}\right)\frac{\partial^4 w}{\partial x^2\partial y^2}-D_{22}\frac{\partial^4 w}{\partial y^4}\end{array}\right)+\\ \left(1-\mu^2\nabla^2\right)\left(\begin{array}{c}-I_0\frac{\partial^2 w}{\partial t^2}+I_2\nabla^2\frac{\partial^2 w}{\partial t^2}-k_w w+k_p\left(\frac{\partial^2 w}{\partial x^2}+\frac{\partial^2 w}{\partial y^2}\right)-c_d\frac{\partial w}{\partial t}-\\ \left(N^T+N^H\right)\left(\frac{\partial^2 w}{\partial x^2}+\frac{\partial^2 w}{\partial y^2}\right)+\frac{e_{31}K_cC(t)h_c}{E_c}\frac{\partial^2 u}{\partial x\partial t}+\frac{e_{32}K_cC(t)h_c}{E_c}\frac{\partial^2 v}{\partial y\partial t}\end{array}\right)=0\end{gathered} \tag{42}$$

in which

$$\begin{cases}N^T=\int_{-\frac{h_c}{2}}^{\frac{h_c}{2}}\int_0^b\frac{E_c}{1-\nu_c}\alpha_c\Delta T dydz+\left(\int_{-\frac{h_c}{2}}^{-\frac{(h_c+h_f)}{2}}\int_0^b\frac{E_f}{1-\nu_f}\alpha_f\Delta T dydz+\int_{\frac{h_c}{2}}^{\frac{(h_c+h_f)}{2}}\int_0^b\frac{E_f}{1-\nu_f}\alpha_f\Delta T dydz\right)\\ N^H=\int_{-\frac{h_c}{2}}^{\frac{h_c}{2}}\int_0^b\frac{E_c}{1-\nu_c}\beta_c\Delta C dydz+\left(\int_{-\frac{h_c}{2}}^{-\frac{(h_c+h_f)}{2}}\int_0^b\frac{E_f}{1-\nu_f}\beta_f\Delta C dydz+\int_{\frac{h_c}{2}}^{\frac{(h_c+h_f)}{2}}\int_0^b\frac{E_f}{1-\nu_f}\beta_f\Delta C dydz\right)\end{cases} \tag{43}$$

In above relation, α_c, α_f, β_c, and β_f correspond with the thermal and moisture expansion coefficients of core and face sheets, respectively.

2.4 Analytical solution

Here, an analytical solution method is applied to solve the governing equations. The details of the wave propagation analysis can be more realized by studying the complementary references about the wave propagation responses of composite plates (Yahia *et al*. 2015). The displacements are supposed to be as

$$\begin{Bmatrix}u\\v\\w\end{Bmatrix}=\begin{Bmatrix}U\exp\left[i\left(\beta_1 x+\beta_2 y-\omega t\right)\right]\\V\exp\left[i\left(\beta_1 x+\beta_2 y-\omega t\right)\right]\\W\exp\left[i\left(\beta_1 x+\beta_2 y-\omega t\right)\right]\end{Bmatrix} \tag{44}$$

Table 1 Material properties of Terfenol-D

E_c (GPa)	ν_c	ρ_c (kg/m^3)	α_c (1/K)	$e_{31}=e_{32}$ (N/mA)
30	0.25	9250	12e-6	442.55

Table 2 Material properties of Alumina (Al_2O_3)

E_f (GPa)	ν_f	ρ_f (kg/m^3)	α_f (1/K)	β_f (wt. % H_2O)$^{-1}$
380	0.3	3800	7e-6	0.0001

where U, V and W are wave amplitudes, β_1 and β_2 are wave numbers in x and y directions, respectively; and ω is the circular frequency of dispersed waves. Substituting for u, v and w from Eq. (44) in the Eqs. (40)-(42), the following equation is obtained

$$\left(\left[K\right]+i\omega\left[C\right]-\omega^2\left[M\right]\right)\begin{bmatrix}U\\V\\W\end{bmatrix}=\begin{bmatrix}0\\0\\0\end{bmatrix} \tag{45}$$

Solving the above equation results in finding the circular frequency. Once this value is divided by wave number, the phase velocity can be reached as

$$c_p=\frac{\omega}{\beta} \tag{46}$$

3. Results and discussion

In this part, the wave dispersion behaviors of a MSNP are going to be reviewed numerically in order to understand the effect of various parameters. In the present article, central core is presumed to be made of Terfenol-D and the top and bottom face sheets are supposed to be consisted of Alumina. The properties of constituent materials are presented in Tables 1 and 2. Moreover, in Table 3 results of verification are presented which show the accuracy and efficiency of present approach.

In Fig. 2, variation of wave frequency versus wave number for various nonlocal and length scale parameters is depicted to put emphasize on the crucial impact of these coefficients on the dispersion responses of MSNPs. It can be figured out that the wave frequency amounts can be decreased whenever nonlocality is increased from zero to a desirable nonzero value in the case of NE (λ = 0). Therefore, the stiffness-softening influence can be easily found in this diagram which is the reduction of wave frequency while nonlocal parameter is added. On the other hand, in a certain nonzero amount of nonlocal parameter

Table 3 Comparison of first dimensionless fundamental frequencies of functionally graded nanoplates with respect to nonlocality, plate's thickness and aspect ratio (n = 5, a = 10 nm)

a/b	μ (nm^2)	a/h = 10		a/h = 20	
		Present	Natarajan *et al*. (2012)	Present	Natarajan *et al*. (2012)
1	0	0.0461	0.0441	0.0116	0.0113
	1	0.0422	0.0403	0.0106	0.0103
	2	0.0391	0.0374	0.0098	0.0096
	4	0.0345	0.0330	0.0086	0.0085
2	0	0.1137	0.1055	0.0288	0.0279
	1	0.0930	0.0863	0.0235	0.0229
	2	0.0806	0.0748	0.0204	0.0198
	4	0.0659	0.0612	0.0167	0.0162

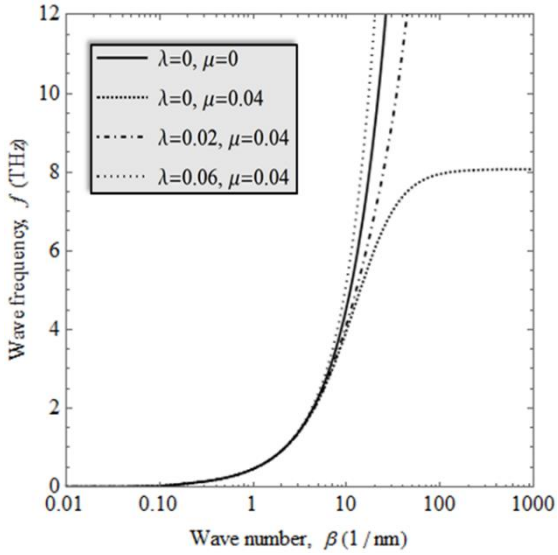

Fig. 2 Variation of wave frequency of MSNPs for different amounts of nonlocal and length scale parameters (k_w = 0.01, k_p = 0.05, c_d = 0, ΔT = 100, ΔC = 0)

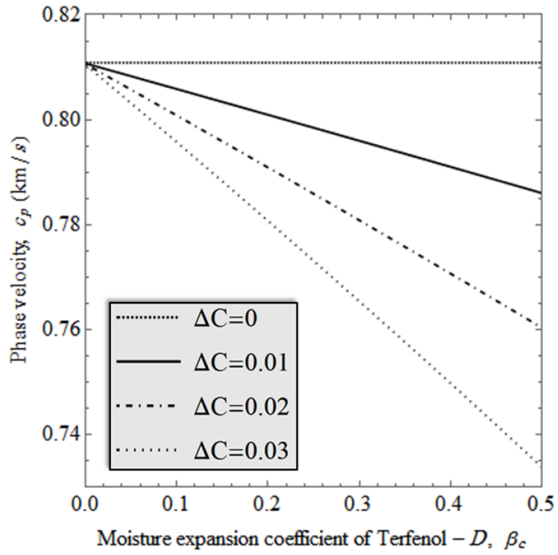

Fig. 3 Influence of moisture expansion coefficient of magnetostrictive core on the phase velocity of MSNPs for various moisture concentration values (k_w = 0.01, k_p = 0.05, c_d = 0.1, ΔT = 100, β = 0.05 (1/nm), $\lambda = \mu$)

(μ = constant), a rise in the magnitude of wave frequency can be reported as length scale parameter is supposed to be intensified. Thus, length scale parameter is able to aggrandize the value of dispersion answers of MSNPs once it is motivated increasingly. The reason of this phenomenon is exactly the hardening effect of the length scale term on the mechanical responses of nanostructures. Afterwards, Fig. 3 is mainly rendered for the purpose of showing the effect of moisture expansion coefficient of Terfenol-D on the phase velocity values of MSNPs whenever moisture concentration is assumed to be varied. In fact, there is a lack of information about the moisture expansion coefficient of

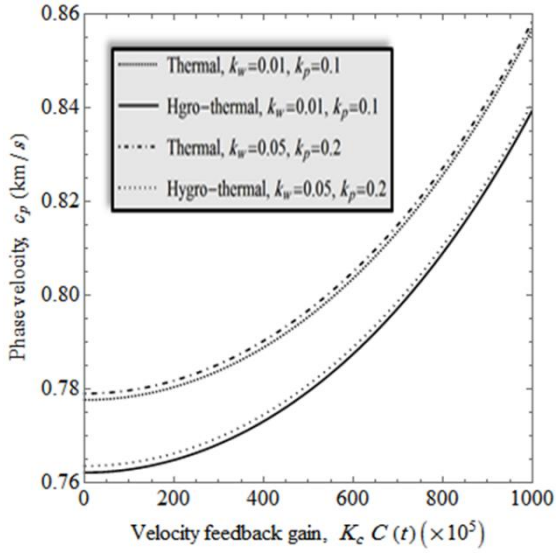

Fig. 4 Effect of velocity feedback gain on the phase velocity of MSNPs under various hygro-thermal loadings and medium conditions (β = 0.03, $\lambda = \mu$, c_d = 0.2)

this smart material. However, it is clear that Terfenol-D is consisted of Terbium, Iron and Dysprosium which are metallic materials. Hence, moisture expansion coefficient of Terfenol-D should be in the routine range of this coefficient for metals. In this figure, this coefficient is considered to be varied from 0 to 0.5 and the influences of gradual changes in this coefficient on the wave dispersion speed are observed. Based on the diagram, a linear impact with negative slope can be seen for moisture expansion coefficient whenever a nonzero amount is employed for moisture concentration ($\Delta C \neq 0$). In other words, in the cases of moist environments phase velocity decreases continuously as moisture expansion coefficient of Terfenol-D increases, whereas, it remains constant in dry situations. From now, in all of the future diagrams, the desirable value of 0.3 is aligned to the moisture expansion coefficient of Terfenol-D (β_c = 0.3 (*wt.* % H_2O)$^{-1}$).

Furthermore, in Fig. 4 influence of velocity feedback gain on the phase velocity of MSNPs is taken into consideration for various environments and different values of foundation parameters. Clearly, it can be observed that phase velocity can be controlled by changing velocity feedback gain amounts. Indeed, once this control gain is added, phase velocity of MSNPs becomes greater. On the other hand, it can be perceived that the wave speed grows in the cases of higher Winkler and Pasternak foundations. Also, it is of interest that phase velocity values are bigger under thermal loading compared to the condition in which the structure is placed in a hygro-thermal environment. So, the decreasing effect of moisture concentration can be easily found again in this figure as same as Fig. 3.

Fig. 5 is plotted to show the effects of various environments on the phase velocity of MSNPs with respect to the medium's damping coefficient for various wave numbers. First of all, it is clear that wave dispersion responses go through a continuous decreasing path as damping coefficient increases; however, value of critical damping coefficient which results in the zero value for

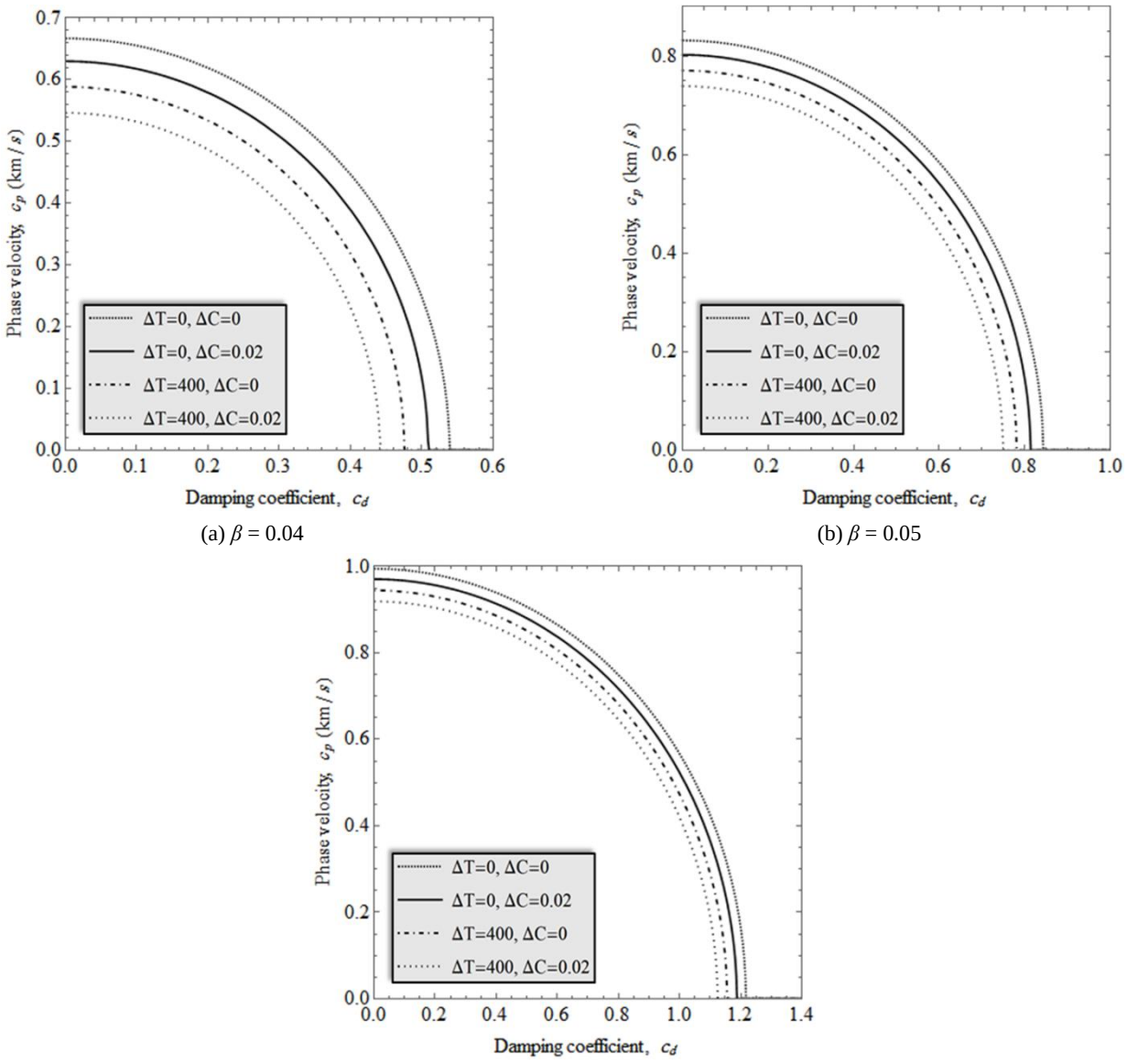

(a) β = 0.04 (b) β = 0.05

(c) β = 0.06

Fig. 5 Variation of phase velocity versus damping coefficient for various temperature rise and moisture concentration values (k_w = 0.01, k_p = 0.05, $\lambda = \mu$)

phase velocity is not constant for all wave numbers. In other words, greater damping coefficients are needed to totally damp the phase velocity of dispersed waves whenever a high wave number is employed. Therefore, in the design procedures, dampers with higher viscosities shall be utilized if high wave numbers are applied. On the other hand, based on the figure, any increase in either temperature rise or moisture concentration leads to smaller wave velocities. Thus, smaller damping coefficients can be used once the system is placed in hygro-thermal and thermal environments compared to the condition of non-hygro-thermal environments.

At last, coupled effects of moisture concentration, temperature rise and foundation parameters are investigated in Fig. 6 drawing the variations of phase velocity versus moisture concentration. Herein, it is obvious that phase velocity values become greater once higher foundation parameters are chosen. Moreover, it can be understood that a rise in the moisture concentration results in a decrease in the value of phase velocity. Also, a same impact can be reported for probable changes in the temperature rise; means, the maximum amount of phase velocity is a desired moisture concentration can be reached in the case of $\mathbf{\Delta}$T = 0. So, in the cases that there is a limitation for moisture concentration, higher temperature rises can be utilized instead.

4. Conclusions

Present paper is an analytical method for wave propagation analysis of MSNPs in hygro-thermal environments. In this model, a NSG based plate model is introduced to probe the size effects in details. The magnetostriction effects are covered on the basis of a feedback control system. Nanoplate is rested on a

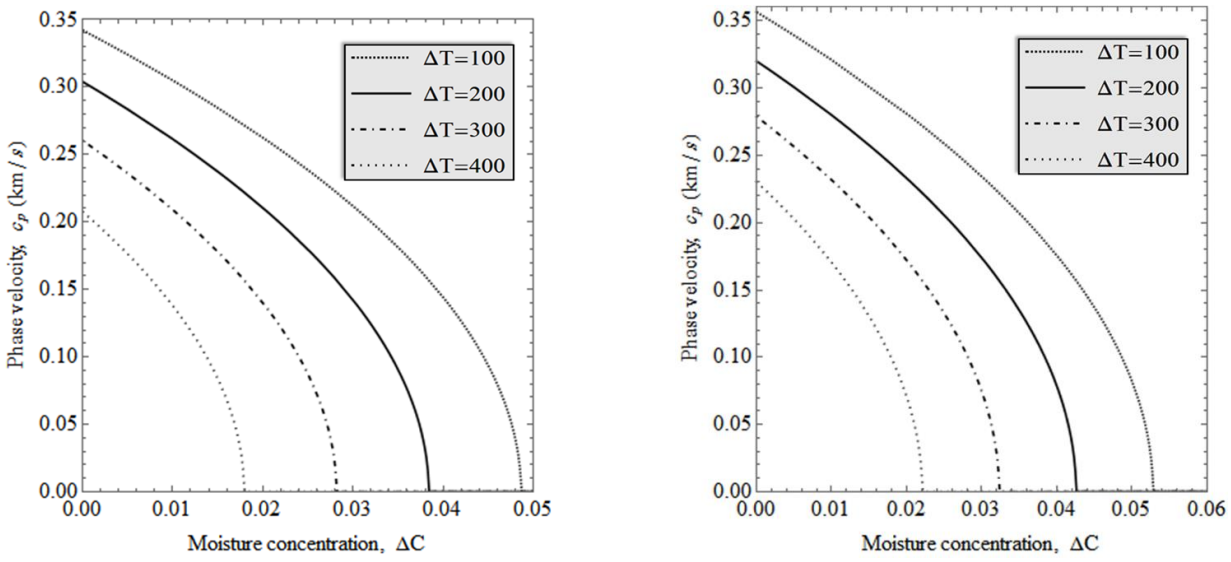

(a) k_w = 0.01, k_p = 0.05 (b) k_w = 0.1, k_p = 0.5

Fig. 6 Variation of phase velocity versus moisture concentration for various amounts of temperature rise and foundation parameters (β = 0.04, $\lambda = \mu$, c_d = 0.2)

viscoelastic substrate and modeled by a CPT. On the other hand, governing equations are developed according to the Hamilton's principle. Herein, a summary of most significant results is presented as follows:

- Wave dispersion answers of MSNPs can be amplified by either increasing the length scale parameter or decreasing the nonlocal parameter.
- A rise in the amount of velocity feedback gain results in higher phase velocities.
- Utilizing greater Winkler or Pasternak coefficients, phase velocity values can be added.
- Phase velocity of the system decreases once temperature rise or moisture concentration values are amplified or a higher damping coefficient is used.

References

Abdelaziz, H.H., Meziane, M.A.A., Bousahla, A.A., Tounsi, A., Mahmoud, S.R. and Alwabli, A.S. (2017), "An efficient hyperbolic shear deformation theory for bending, buckling and free vibration of fgm sandwich plates with various boundary conditions", *Steel Compos. Struct., Int. J.*, **25**(6), 693-704.

Abualnour, M., Houari, M.S.A., Tounsi, A. and Mahmoud, S.R. (2018), "A novel quasi-3d trigonometric plate theory for free vibration analysis of advanced composite plates", *Compos. Struct.*, **184**, 688-697.

Ahouel, M., Houari, M.S.A., Bedia, E.A. and Tounsi, A. (2016), "Size-dependent mechanical behavior of functionally graded trigonometric shear deformable nanobeams including neutral surface position concept", *Steel Compos. Struct., Int. J.*, **20**(5), 963-981.

Bayat, R., Jafari, A.A. and Rahmani, O. (2015), "Analytical solution for free vibration of laminated curved beam with magnetostrictive layers", *Int. J. Appl. Mech.*, **7**(3), p. 1550050.

Beldjelili, Y., Tounsi, A. and Mahmoud, S.R. (2016), "Hygro-thermo-mechanical bending of s-fgm plates resting on variable elastic foundations using a four-variable trigonometric plate theory", *Smart Struct. Syst., Int. J.*, **18**(4), 755-786.

Bellifa, H., Benrahou, K.H., Bousahla, A.A., Tounsi, A. and Mahmoud, S.R. (2017), "A nonlocal zeroth-order shear deformation theory for nonlinear postbuckling of nanobeams", *Struct. Eng. Mech., Int. J.*, **62**(6), 695-702.

Ebrahimi, F. and Barati, M.R. (2016), "Hygrothermal buckling analysis of magnetically actuated embedded higher order functionally graded nanoscale beams considering the neutral surface position", *J. Thermal Stress.*, **39**(10), 1210-1229.

Ebrahimi, F. and Barati, M.R. (2017), "Through-the-length temperature distribution effects on thermal vibration analysis of nonlocal strain-gradient axially graded nanobeams subjected to nonuniform magnetic field", *J. Thermal Stress.*, **40**(5), 548-563.

Ebrahimi, F. and Barati, M.R. (2018a), "Damping vibration behavior of visco-elastically coupled double-layered graphene sheets based on nonlocal strain gradient theory", *Microsyst. Technol.*, **24**(3), 1643-1658.

Ebrahimi, F. and Barati, M.R. (2018b), "Vibration analysis of graphene sheets resting on the orthotropic elastic medium subjected to hygro-thermal and in-plane magnetic fields based on the nonlocal strain gradient theory", *Proceedings of the Institution of Mechanical Engineers, Part C: Journal of Mechanical Engineering Science*, **232**(13), 2469-2481.

Ebrahimi, F. and Dabbagh, A. (2017a), "Nonlocal strain gradient based wave dispersion behavior of smart rotating magneto-electro-elastic nanoplates", *Mater. Res. Express*, **4**(2), p. 025003.

Ebrahimi, F. and Dabbagh, A. (2017b), "On flexural wave propagation responses of smart fg magneto-electro-elastic nanoplates via nonlocal strain gradient theory", *Compos. Struct.*, **162**, 281-293.

Ebrahimi, F. and Dabbagh, A. (2017c), "Wave propagation analysis of embedded nanoplates based on a nonlocal strain gradient-based surface piezoelectricity theory", *Eur. Phys. J. Plus*, **132**(11), p. 449.

Ebrahimi, F. and Dabbagh, A. (2017d), "Wave propagation analysis of smart rotating porous heterogeneous piezo-electric nanobeams", *Eur. Phys. J. Plus*, **132**(4), p. 153.

Ebrahimi, F. and Dabbagh, A. (2018a), "Effect of humid-thermal environment on wave dispersion characteristics of single-layered graphene sheets", *Appl. Phys. A*, **124**(4), p. 301.

Ebrahimi, F. and Dabbagh, A. (2018b), "On modeling wave

dispersion characteristics of protein lipid nanotubules", *J. Biomech.*, **77**, pp. 1-7.

Ebrahimi, F. and Dabbagh, A. (2018c), "On wave dispersion characteristics of double-layered graphene sheets in thermal environments", *J. Electromag. Waves Appl.*, **32**(15), 1869-1888.

Ebrahimi, F. and Dabbagh, A. (2018d), "Thermo-magnetic field effects on the wave propagation behavior of smart magnetostrictive sandwich nanoplates", *Eur. Phys. J. Plus*, **133**(3), p. 97.

Ebrahimi, F. and Dabbagh, A. (2018e), "Wave dispersion characteristics of orthotropic double-nanoplate-system subjected to a longitudinal magnetic field", *Microsyst. Technol.*, **24**(7), 2929-2939.

Ebrahimi, F. and Dabbagh, A. (2018f), "Wave dispersion characteristics of rotating heterogeneous magneto-electro-elastic nanobeams based on nonlocal strain gradient elasticity theory", *J. Electromag. Waves Appl.*, **32**(2), 138-169.

Ebrahimi, F. and Dabbagh, A. (2018g), "Wave propagation analysis of magnetostrictive sandwich composite nanoplates via nonlocal strain gradient theory", *Proceedings of the Institution of Mechanical Engineers, Part C: Journal of Mechanical Engineering Science*, **232**(22), 4180-4192.

Ebrahimi, F. and Hosseini, S. (2016), "Thermal effects on nonlinear vibration behavior of viscoelastic nanosize plates", *J. Thermal Stress.*, **39**(5), 606-625.

Ebrahimi, F., Salari, E. and Hosseini, S.A.H. (2015), "Thermomechanical vibration behavior of fg nanobeams subjected to linear and non-linear temperature distributions", *J. Thermal Stress.*, **38**(12), 1360-1386.

Ebrahimi, F., Barati, M.R. and Dabbagh, A. (2016a), "A nonlocal strain gradient theory for wave propagation analysis in temperature-dependent inhomogeneous nanoplates", *Int. J. Eng. Sci.*, **107**, 169-182.

Ebrahimi, F., Barati, M.R. and Dabbagh, A. (2016b), "Wave dispersion characteristics of axially loaded magneto-electro-elastic nanobeams", *Appl. Phys. A*, **122**(11), p. 949.

Ebrahimi, F., Dabbagh, A. and Barati, M.R. (2016c), "Wave propagation analysis of a size-dependent magneto-electro-elastic heterogeneous nanoplate", *Eur. Phys. J. Plus*, **131**(12), p. 433.

Ebrahimi, F., Barati, M.R. and Haghi, P. (2017), "Thermal effects on wave propagation characteristics of rotating strain gradient temperature-dependent functionally graded nanoscale beams", *J. Thermal Stress.*, **40**(5), 535-547.

Ebrahimi, F., Barati, M.R. and Dabbagh, A. (2018a), "Wave propagation in embedded inhomogeneous nanoscale plates incorporating thermal effects", *Waves Random Complex Media*, **28**(2), 215-235.

Ebrahimi, F., Haghi, P. and Dabbagh, A. (2018b), "Analytical wave dispersion modeling in advanced piezoelectric double-layered nanobeam systems", *Struct. Eng. Mech., Int. J.*, **67**(2), 175-183.

Eringen, A.C. (1983), "On differential equations of nonlocal elasticity and solutions of screw dislocation and surface waves", *J. Appl. Phys.*, **54**(9), 4703-4710.

Farajpour, A., Yazdi, M.H., Rastgoo, A. and Mohammadi, M. (2016), "A higher-order nonlocal strain gradient plate model for buckling of orthotropic nanoplates in thermal environment", *Acta Mechanica*, **227**(7), pp. 1849-1867.

Fleck, N.A. and Hutchinson, J.W. (1993), "A phenomenological theory for strain gradient effects in plasticity", *J. Mech. Phys. Solids*, **41**(12), 1825-1857.

Ghorbanpour Arani, A., Jamali, M., Ghorbanpour-Arani, A.H., Kolahchi, R. and Mosayyebi, M. (2017), "Electro-magneto wave propagation analysis of viscoelastic sandwich nanoplates considering surface effects", *Proceedings of the Institution of Mechanical Engineers, Part C: Journal of Mechanical Engineering Science*, **231**(2), 387-403.

Hamza-Cherif, R., Meradjah, M., Zidour, M., Tounsi, A., Belmahi, S. and Bensattalah, T. (2018), "Vibration analysis of nano beam using differential transform method including thermal effect", *J. Nano Res.*, **54**, 1-14.

Hong, C. (2009), "Transient responses of magnetostrictive plates without shear effects", *Int. J. Eng. Sci.*, **47**(3), 355-362.

Hosseini-Hashemi, S., Zare, M. and Nazemnezhad, R. (2013), "An exact analytical approach for free vibration of mindlin rectangular nano-plates via nonlocal elasticity", *Compos. Struct.*, **100**, 290-299.

Houari, M.S.A., Tounsi, A., Bessaim, A. and Mahmoud, S.R. (2016), "A new simple three-unknown sinusoidal shear deformation theory for functionally graded plates", *Steel Compos. Struct., Int. J.*, **22**(2), 257-276.

Kaci, A., Houari, M.S.A., Bousahla, A.A., Tounsi, A. and Mahmoud, S.R. (2018), "Post-buckling analysis of shear-deformable composite beams using a novel simple two-unknown beam theory", *Struct. Eng. Mech., Int. J.*, **65**(5), 621-631.

Karami, B., Janghorban, M. and Tounsi, A. (2018), "Variational approach for wave dispersion in anisotropic doubly-curved nanoshells based on a new nonlocal strain gradient higher order shell theory", *Thin-Wall. Struct.*, **129**, 251-264.

Karami, B., Shahsavari, D., Karami, M. and Li, L. (2019), "Hygrothermal wave characteristic of nanobeam-type inhomogeneous materials with porosity under magnetic field", *Proceedings of the Institution of Mechanical Engineers, Part C: Journal of Mechanical Engineering Science*, **233**(6), 2149-2169.

Li, L. and Hu, Y. (2015), "Buckling analysis of size-dependent nonlinear beams based on a nonlocal strain gradient theory", *Int. J. Eng. Sci.*, **97**, 84-94.

Li, L., Tang, H. and Hu, Y. (2018a), "The effect of thickness on the mechanics of nanobeams", *Int. J. Eng. Sci.*, **123**, 81-91.

Li, L., Tang, H. and Hu, Y. (2018b), "Size-dependent nonlinear vibration of beam-type porous materials with an initial geometrical curvature", *Compos. Struct.*, **184**, 1177-1188.

Lim, C.W., Zhang, G. and Reddy, J.N. (2015), "A higher-order nonlocal elasticity and strain gradient theory and its applications in wave propagation", *J. Mech. Phys. Solids*, **78**, 298-313.

Mouffoki, A., Bedia, E.A., Houari, M.S.A., Tounsi, A. and Mahmoud, S.R. (2017), "Vibration analysis of nonlocal advanced nanobeams in hygro-thermal environment using a new two-unknown trigonometric shear deformation beam theory", *Smart Struct. Syst., Int. J.*, **20**(3), 369-383.

Natarajan, S., Chakraborty, S., Thangavel, M., Bordas, S. and Rabczuk, T. (2012), "Size-dependent free flexural vibration behavior of functionally graded nanoplates", *Computat. Mater. Sci.*, **65**, 74-80.

Reddy, J.N. and Barbosa, J.I. (2000), "On vibration suppression of magnetostrictive beams", *Smart Mater. Struct.*, **9**(1), p. 49.

Stölken, J.S. and Evans, A.G. (1998), "A microbend test method for measuring the plasticity length scale", *Acta Materialia*, **46**(14), 5109-5115.

Tang, H., Li, L., Hu, Y., Meng, W. and Duan, K. (2019), "Vibration of nonlocal strain gradient beams incorporating poisson's ratio and thickness effects", *Thin-Wall. Struct.*, **137**, 377-391.

Xiao, W., Li, L. and Wang, M. (2017), "Propagation of in-plane wave in viscoelastic monolayer graphene via nonlocal strain gradient theory", *Appl. Phys. A*, **123**(6), p. 388.

Yahia, S.A., Atmane, H.A., Houari, M.S.A. and Tounsi, A. (2015), "Wave propagation in functionally graded plates with porosities using various higher-order shear deformation plate theories", *Struct. Eng. Mech., Int. J.*, **53**(6), 1143-1165.

Yan, J.W., Tong, L.H., Li, C., Zhu, Y. and Wang, Z.W. (2015), "Exact solutions of bending deflections for nano-beams and nano-plates based on nonlocal elasticity theory", *Compos. Struct.*, **125**, 304-313.

Yifeng, Z., Lei, C., Yu, W. and Xiaoping, Z. (2013), "Variational asymptotic micromechanics modeling of heterogeneous magnetostrictive composite materials", *Compos. Struct.*, **106**, 502-509.

Zaoui, F.Z., Ouinas, D. and Tounsi, A. (2019), "New 2d and quasi-3d shear deformation theories for free vibration of functionally graded plates on elastic foundations", *Compos. Part B: Eng.*, **159**, 231-247.

Zidi, M., Houari, M.S.A., Tounsi, A., Bessaim, A. and Mahmoud, S.R. (2017), "A novel simple two-unknown hyperbolic shear deformation theory for functionally graded beams", *Struct. Eng. Mech., Int. J.*, **64**(2), 145-153.

CC